Supporting Information

Synthesis of Quasi-MOF featured with special hub-and-spoke channels and surface NiO species for enhanced total hydrogenation of furfural

Qiuju Fu[a,b], Liting Yan[a] , Lingzhi Yang[c]*, Dandan Liu[b], Shuo Zhang[b], Huimin Jiang[b], Wenpeng Xie[b], Haiyan Wang[d]* and Xuebo Zhao[a,b]*

[a] *School of Materials Science and Engineering, Qilu University of Technology (Shandong Academy of Sciences), Jinan 250353 (P.R. China)*

[b] *College of Chemistry and Chemical Engineering, China University of Petroleum (East China), Qingdao 266580, (P.R. China)*

[c] *School of Science and Engineering, The Chinese University of Hong Kong, Shenzhen 518172 (P.R. China)*

[d] *School of Petrochemical Engineering, Liaoning Petrochemical University, Liaoning 113001, (P.R. China)*

E-mail addresses: zhaoxuebo@upc.edu.cn (X. Zhao).

Experimental

Materials.

2, 5-dihydroxyterephthalic acid (denoted as dhtp, 98%) was purchased from Aladdin Chemicals. Nickel acetate tetrahydrate ($Ni(OAc)_2 \cdot 4H_2O$, 98%), ethanol (99.7%) and furfural (FFR, 99%) were purchased from Sinopharma Chemical Reagent Co. Ltd (SCRC). Furfuryl alcohol (FFA, 99%) and tetrahydrofurfuryl alcohol (THFA, 99%) were obtained from Damas-beta Chemicals. Deionized water (DIW) was used in all experiments. All the reagents were used without further purification.

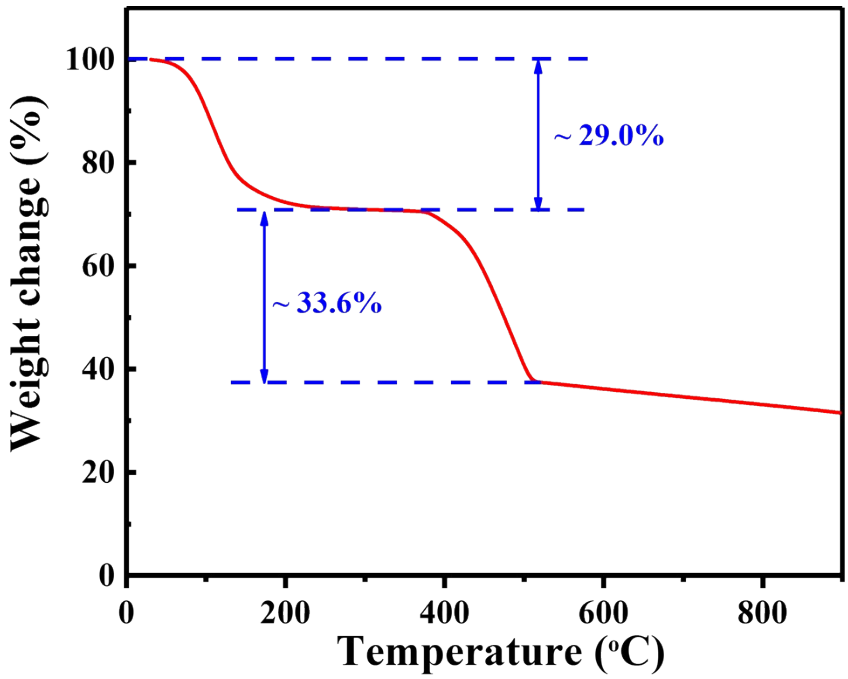

Fig. S1 TG of Ni-MOF-74 with ramp rate of 10 °C·min^{-1} in N_2 atmosphere.

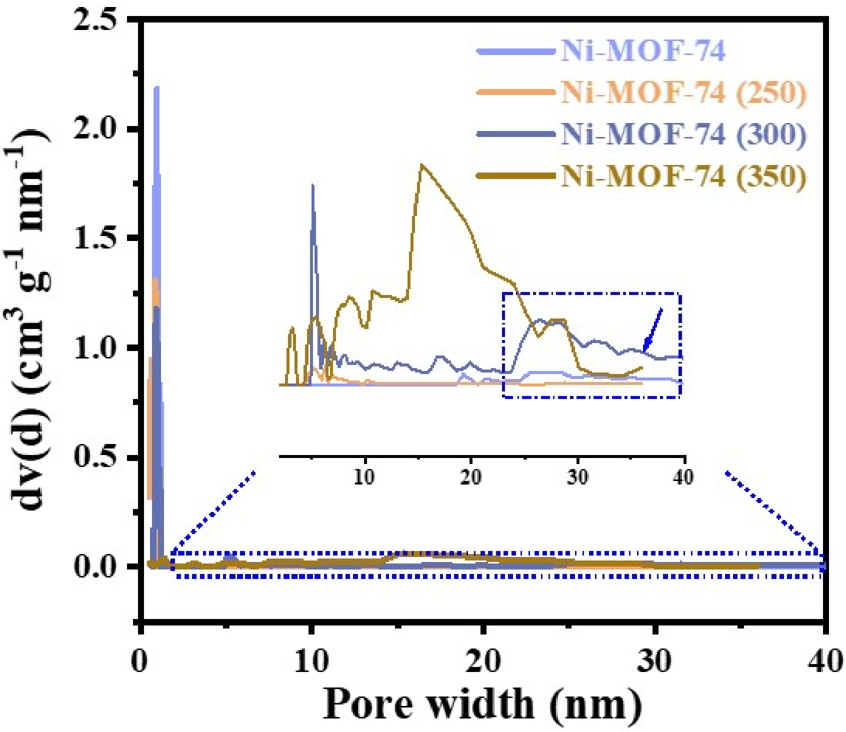

Fig. S2 Pore size distribution at 77 K of Ni-MOF-74 and Ni-MOF-74 (T) samples.

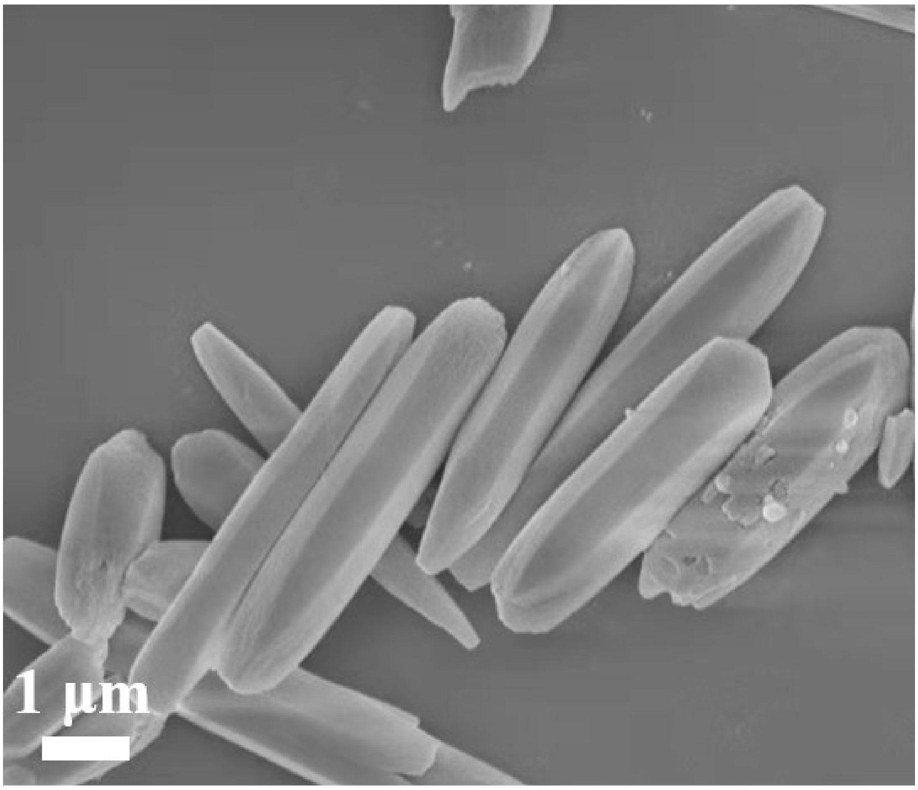

Fig. S3 SEM image of Ni-MOF-74 precursor.

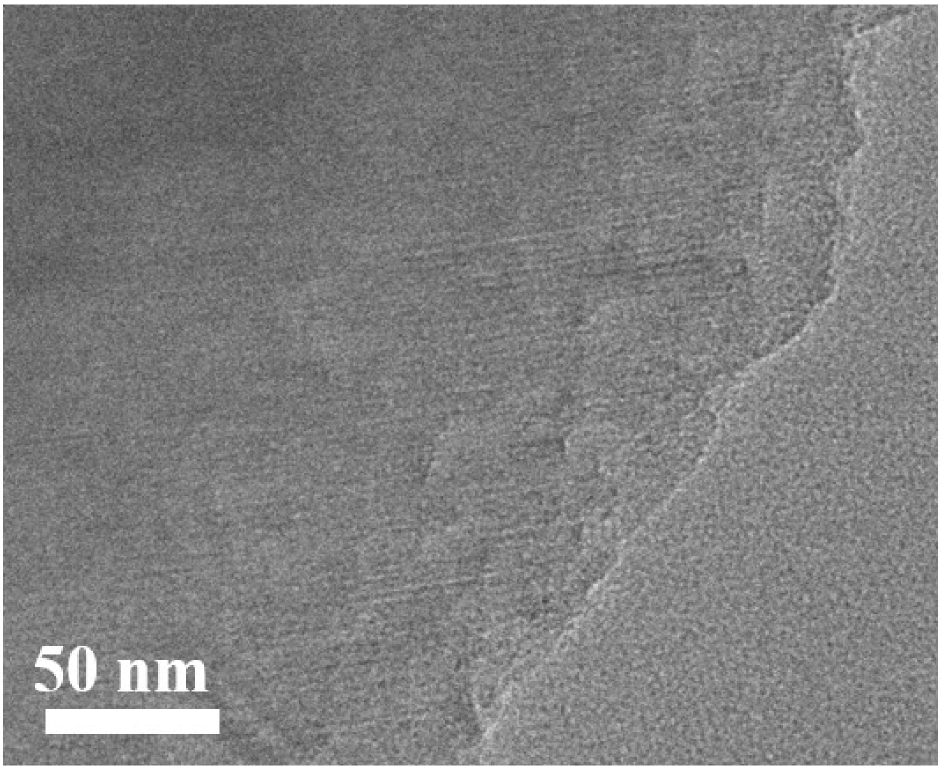

Fig. S4 TEM image of Ni-MOF-74 precursor.

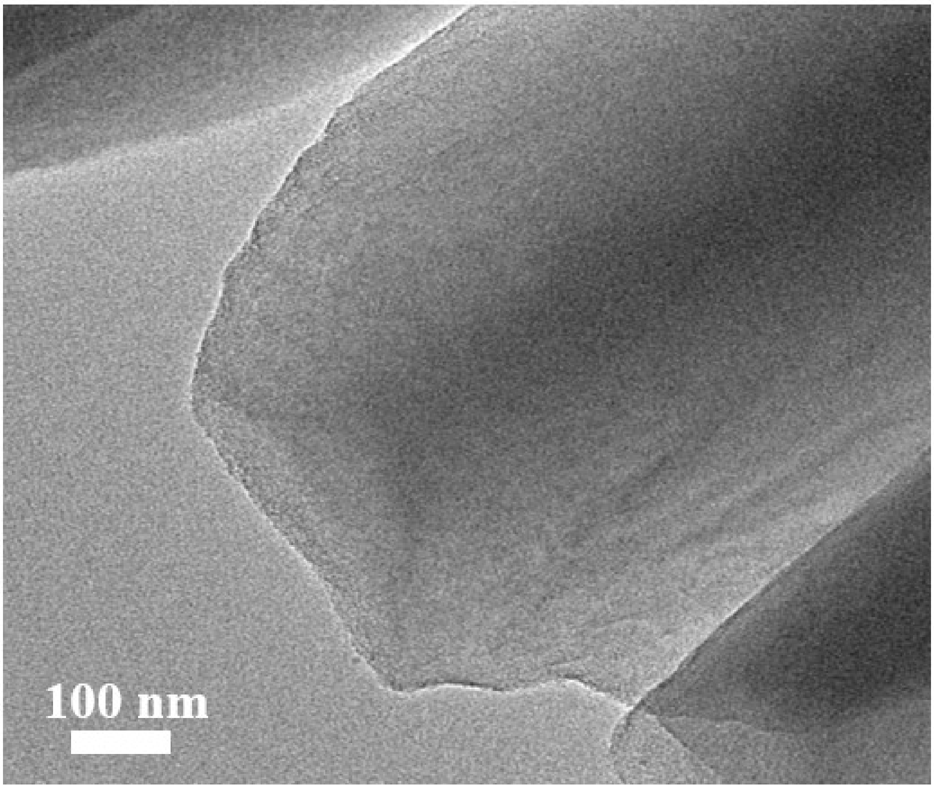

Fig. S5 TEM of Ni-MOF-74 (250) sample.

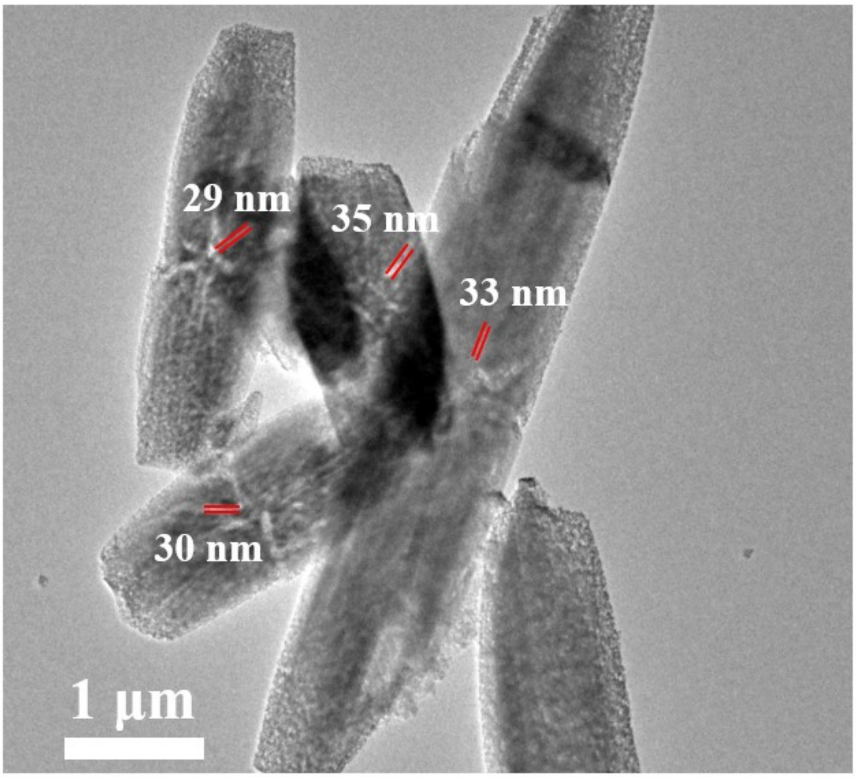

Fig. S6 TEM of Ni-MOF-74 (300) sample.

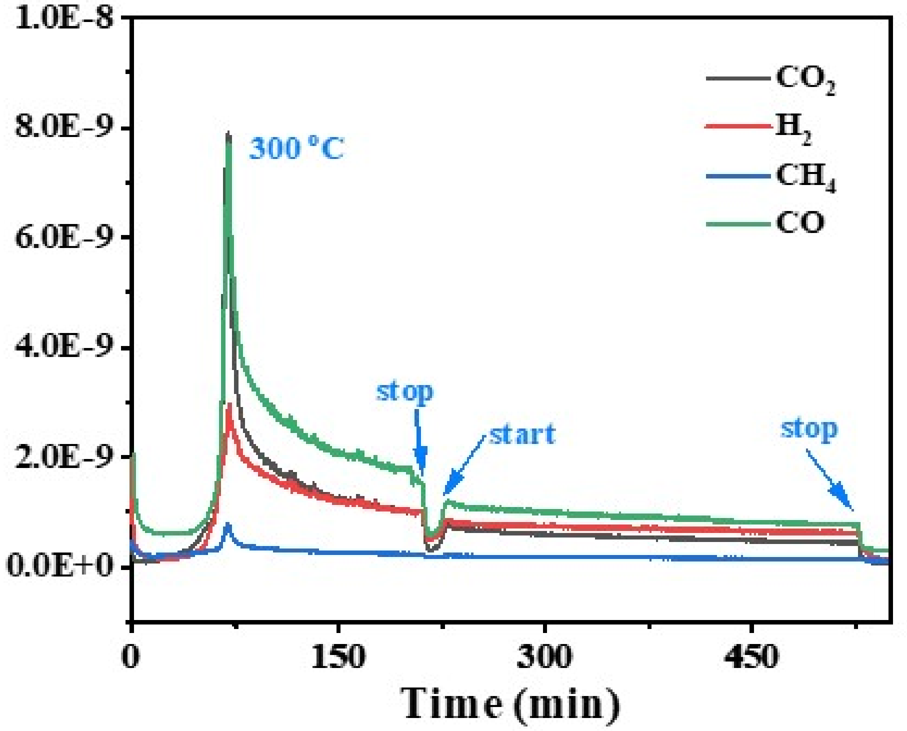

Fig. S7 The decomposition process of Ni-MOF-74 monitored by mass spectrometry from room temperature to 300 °C at a rate of 5 °C·min^{-1}.

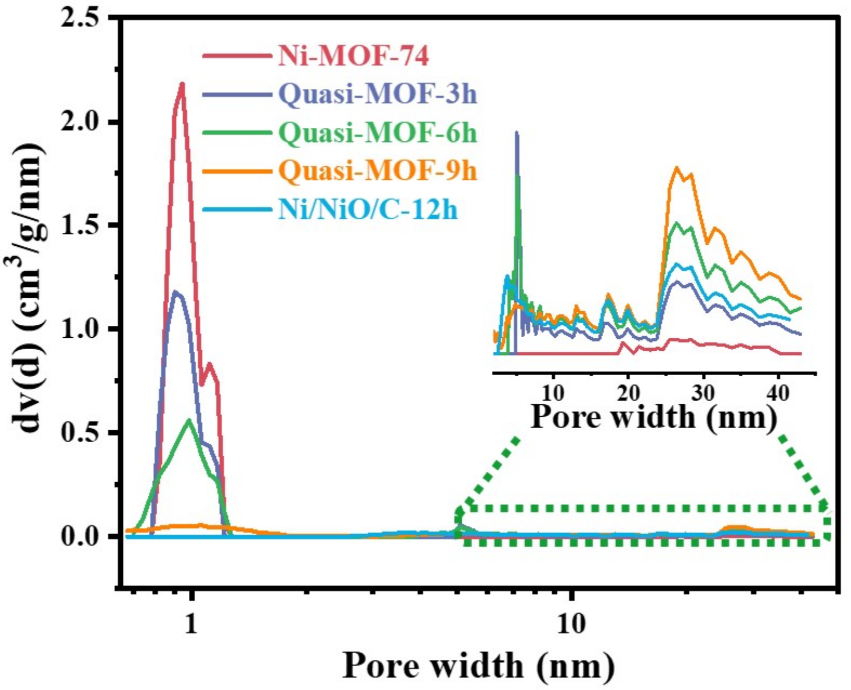

Fig. S8 Pore size distributions at 77 K of Ni-MOF-74 and the derivants.

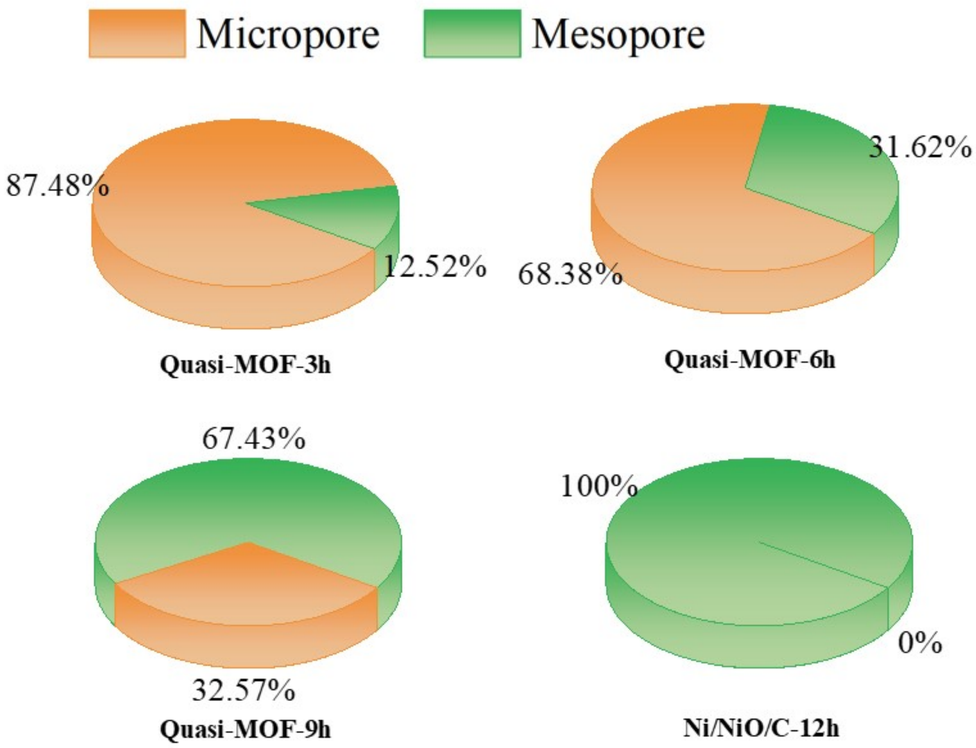

Fig. S9 Percentage of micropore and mesopore of Ni-MOF-74 derivatives.

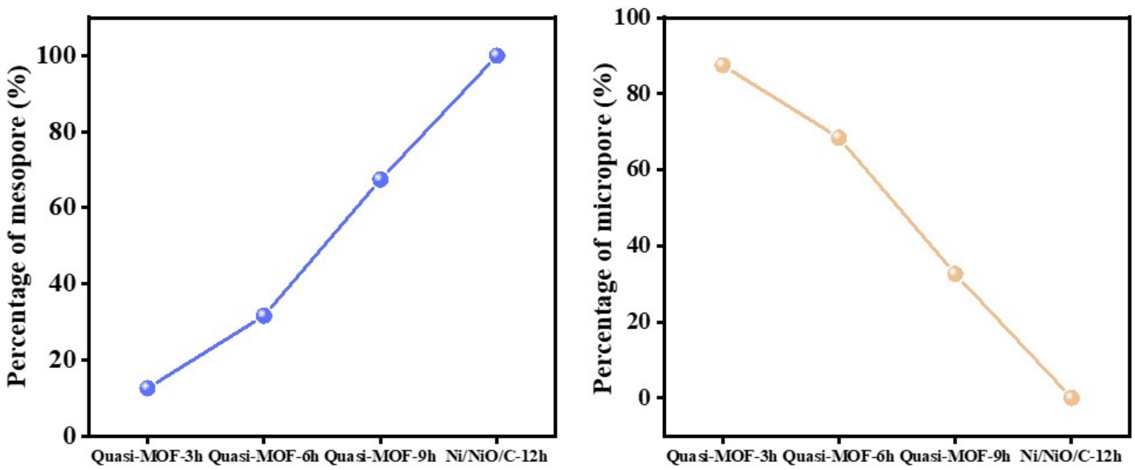

Fig. S10 Changes of micropore and mesopore of Ni-MOF-74 derivatives.

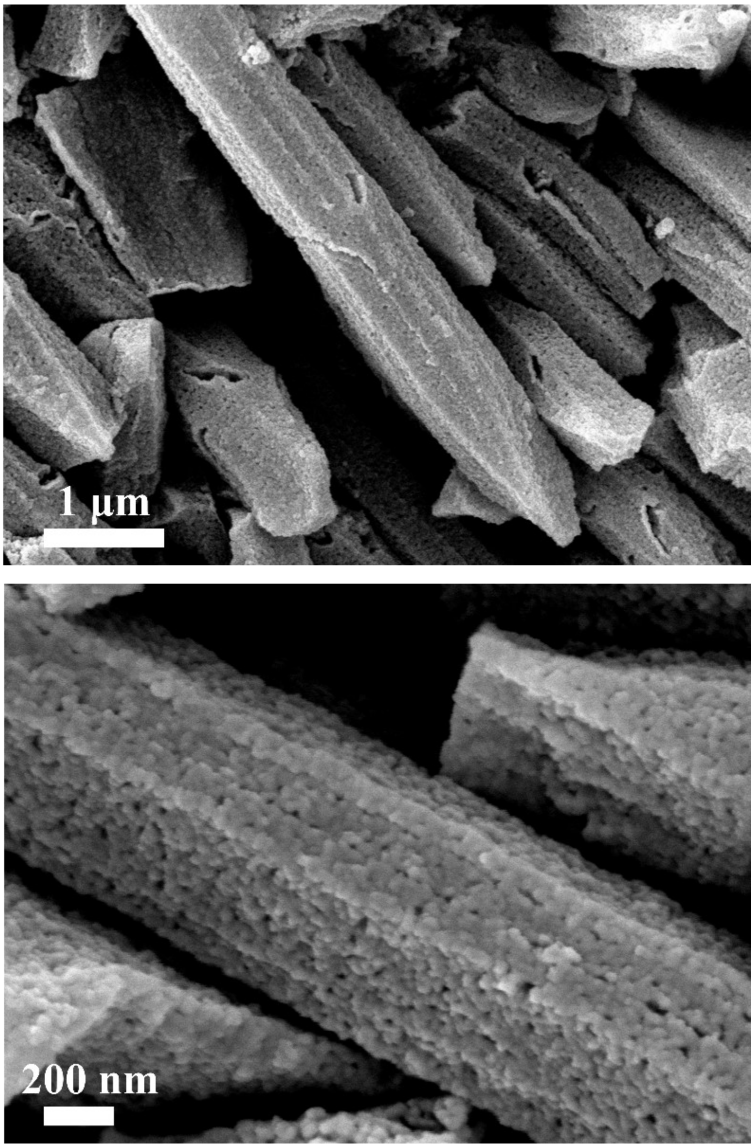

Fig. S11 SEM of Ni/NiO/C-12h sample.

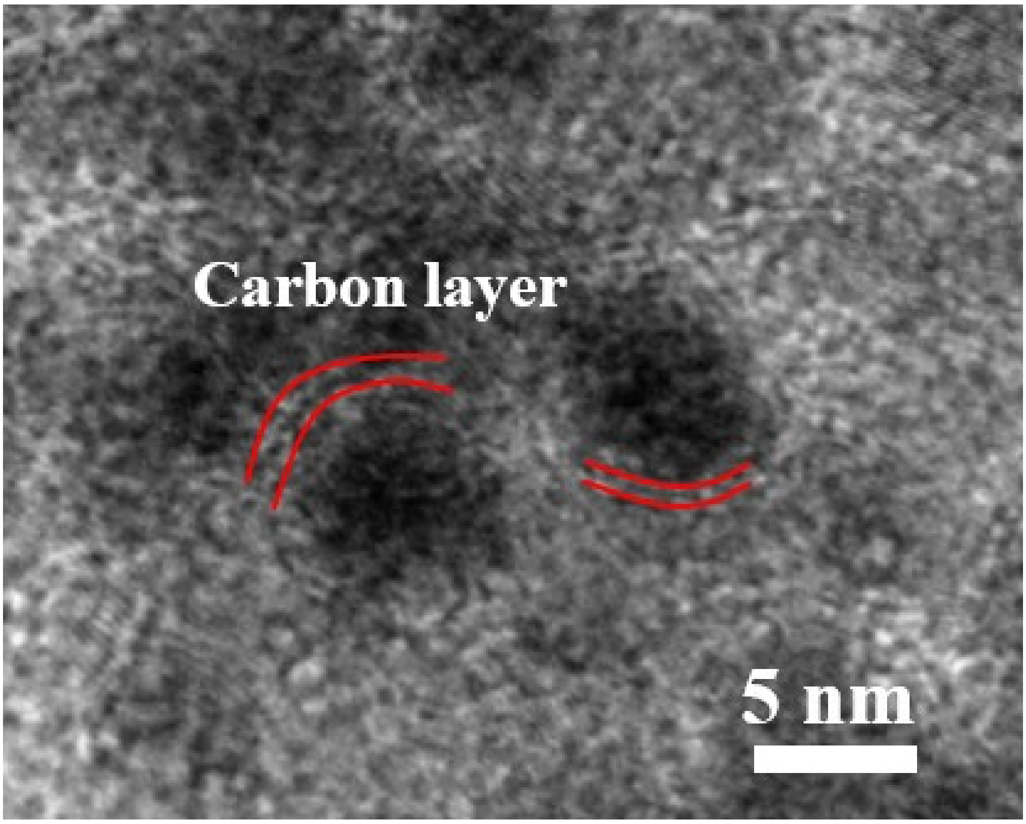

Fig. S12 HRTEM of Quasi-MOF-9h sample.

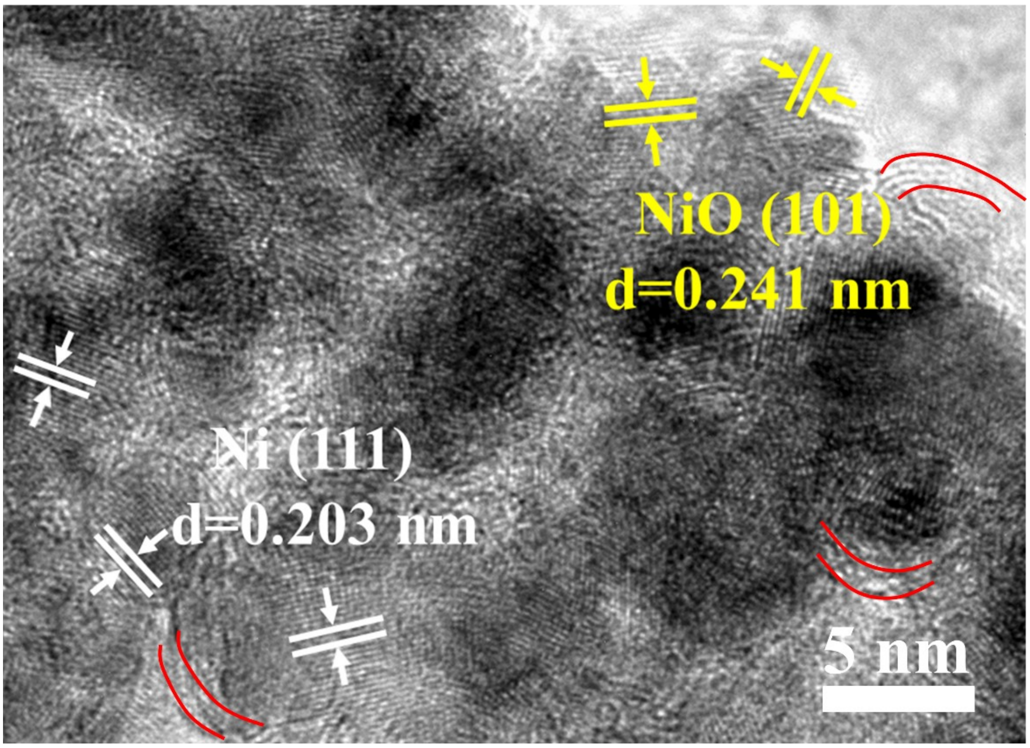

Fig. S13 HRTEM of Ni/NiO/C-12h sample.

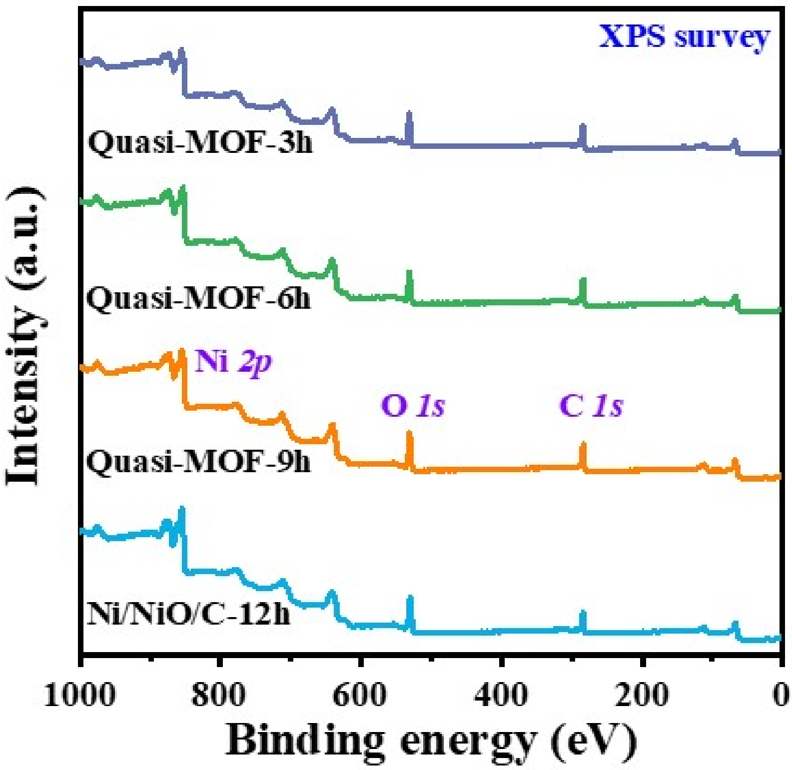

Fig. S14 XPS spectra of survey scan.

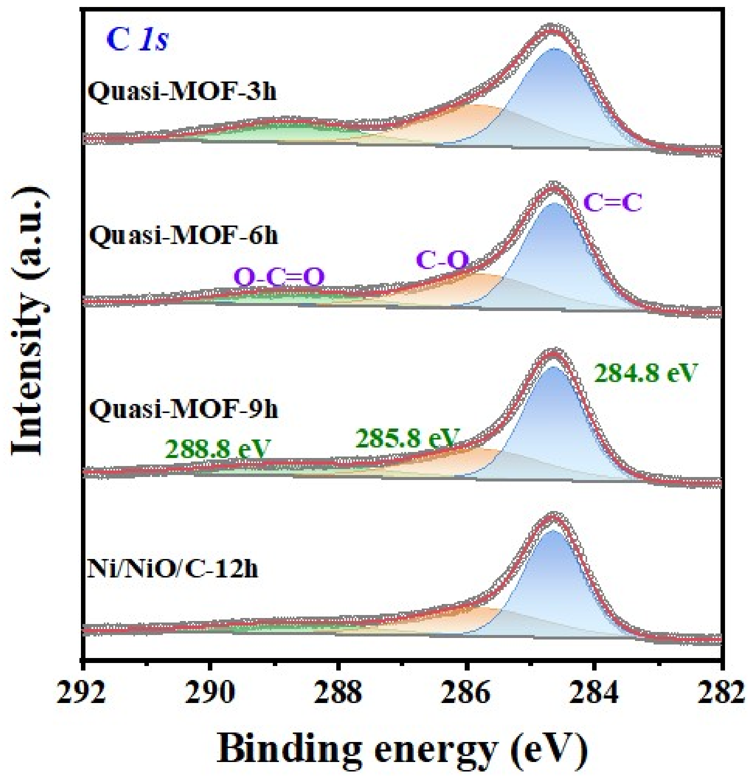

Fig. S15 C 1s spectra of Quasi-MOFs and Ni/NiO/C-12h samples.

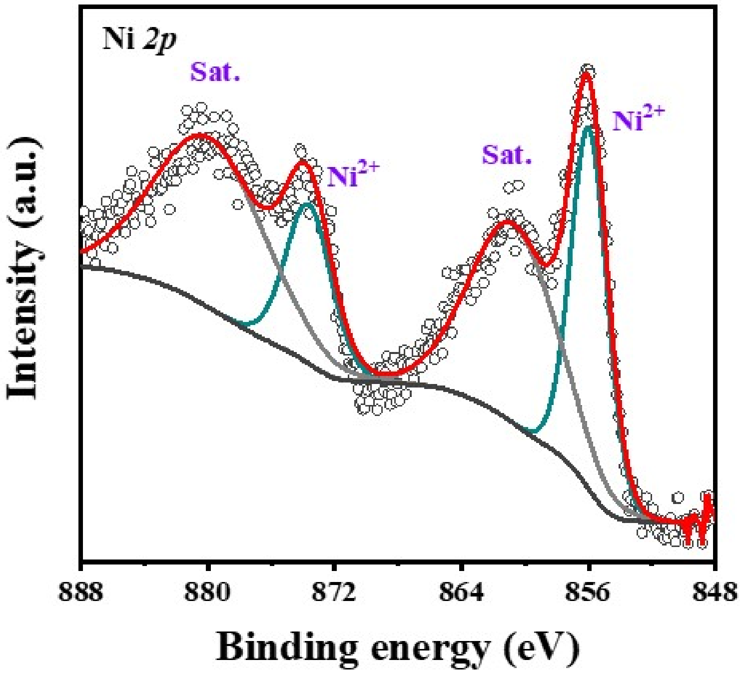

Fig. S16 Ni 2p spectra of Ni-MOF-74 (250) sample.

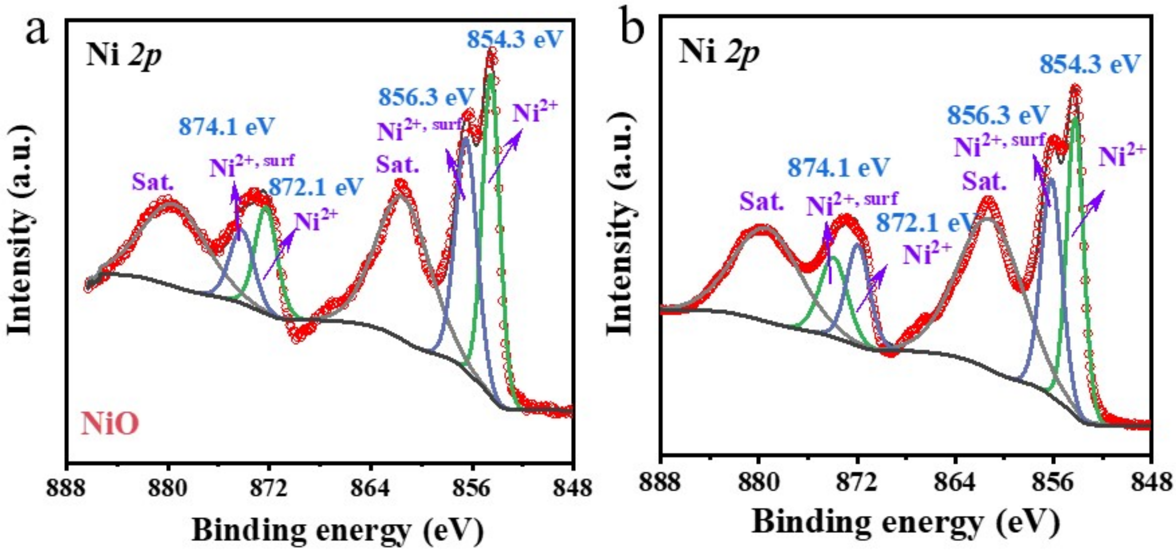

Fig. S17 Ni 2p spectra of a) commercial NiO powder and b) NiO powder prepared by treating $Ni(OAc)_2 \cdot 4H_2O$ at 300 °C under air conditions.

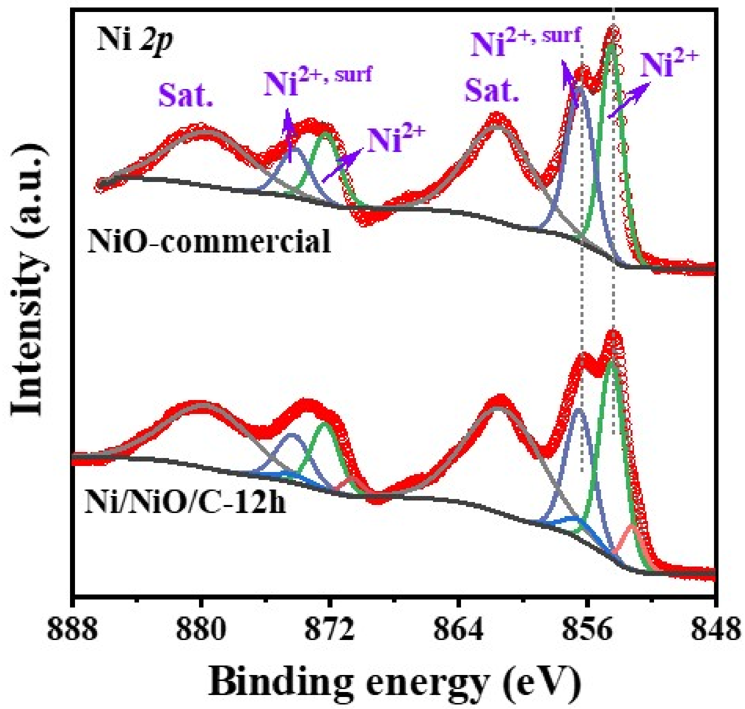

Fig. S18 Ni 2p spectra of Ni-commercial and Ni/NiO/C-12h samples.

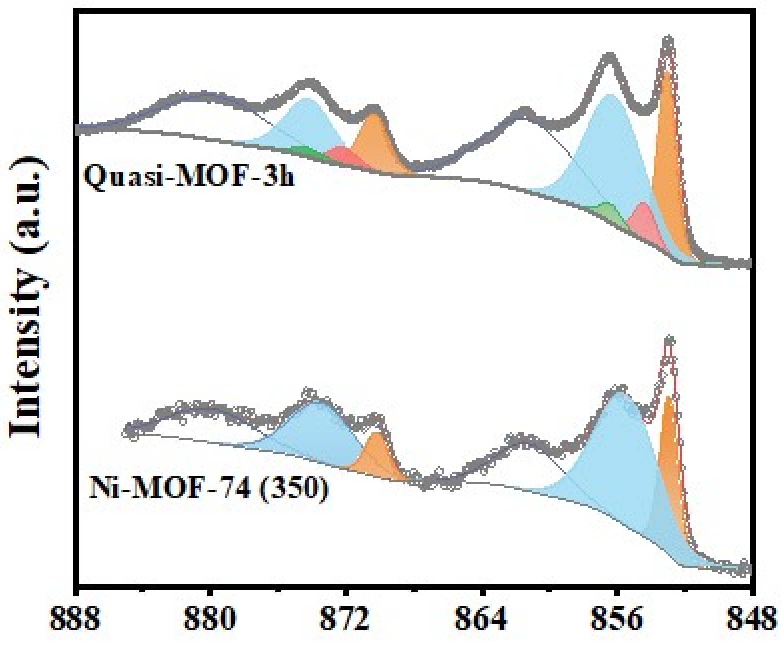

Fig. S19 Ni 2p spectra of Quasi-MOF-3h and Ni-MOF-74 (350) samples.

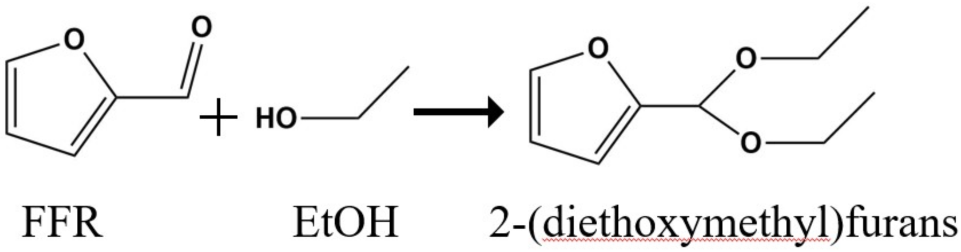

Fig. S20 The condensation reaction route of FFR and ethanol.

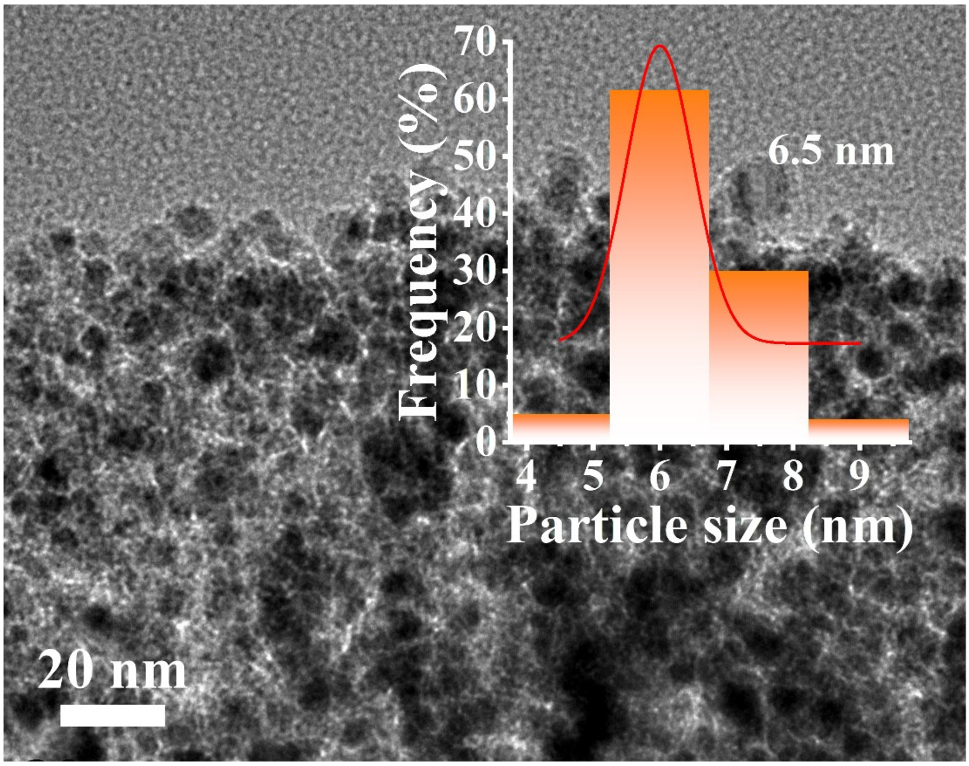

Fig. S21 TEM image of Ni-MOF-74 (350) and corresponding particle size distribution.

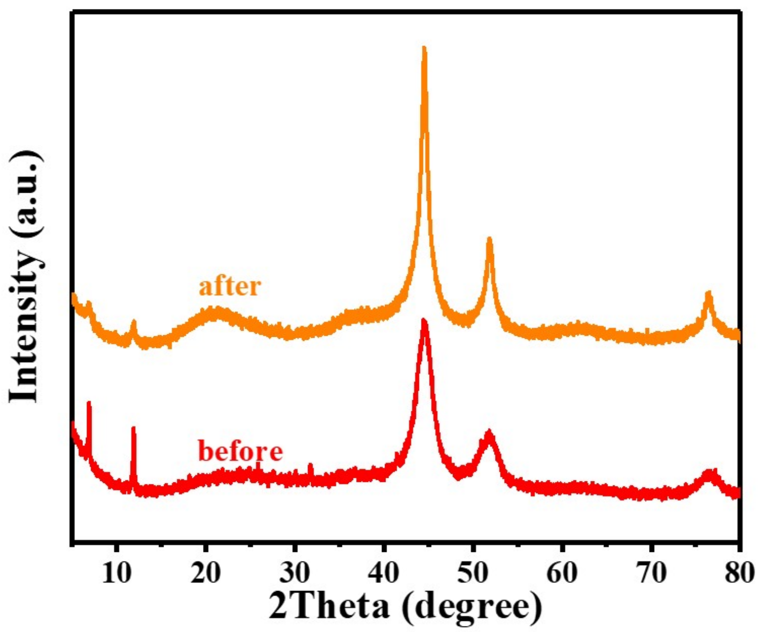

Fig. S22 XRD pattern of Quasi-MOF-9h after five consecutive runs.

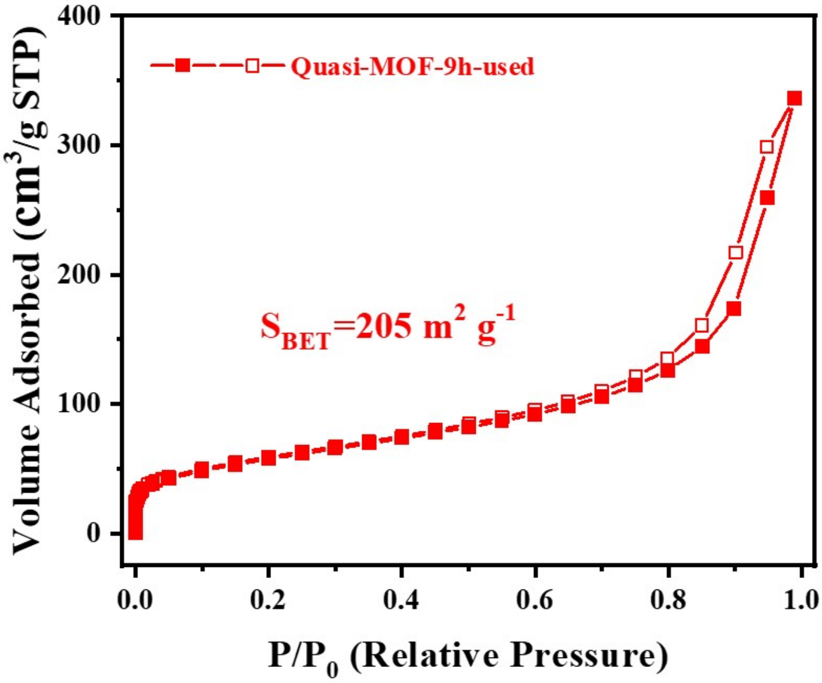

Fig. S23 N_2 adsorption-desorption isotherm at 77 K of Quasi-MOF-9h after five consecutive runs.

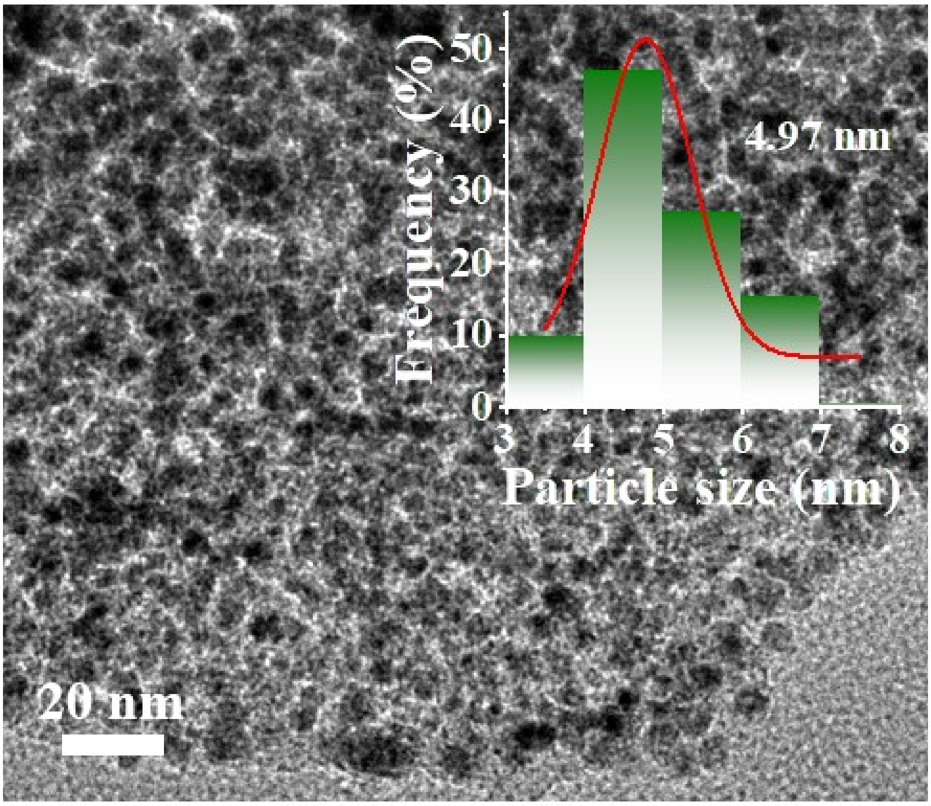

Fig. S24 TEM pattern of Quasi-MOF-9h after five consecutive runs.

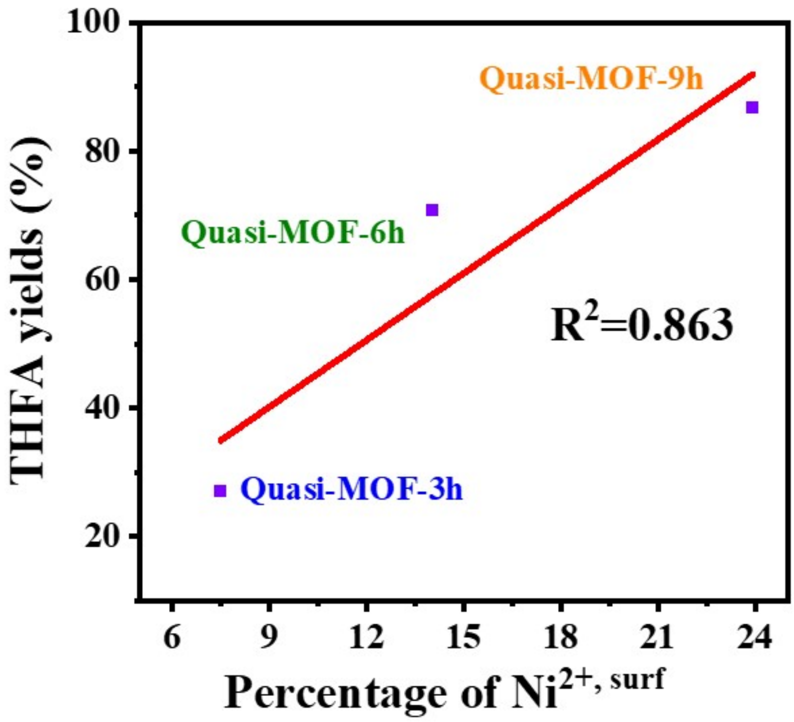

Fig. S25 Correlation between percentage of $Ni^{2+, surf}$ and THFA yields.

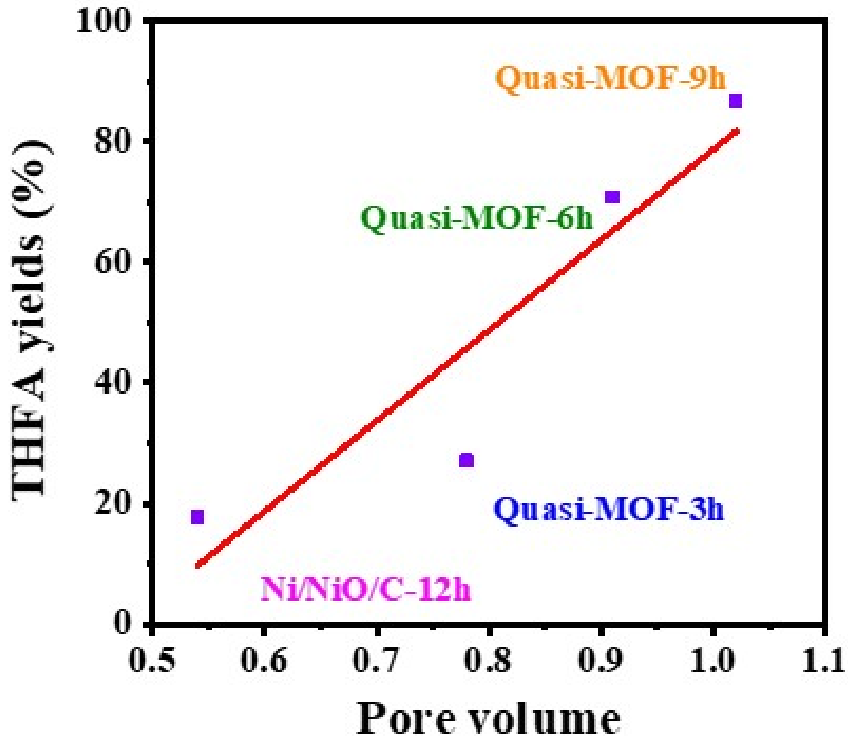

Fig. S26 Correlation between total pore volume and THFA yields.

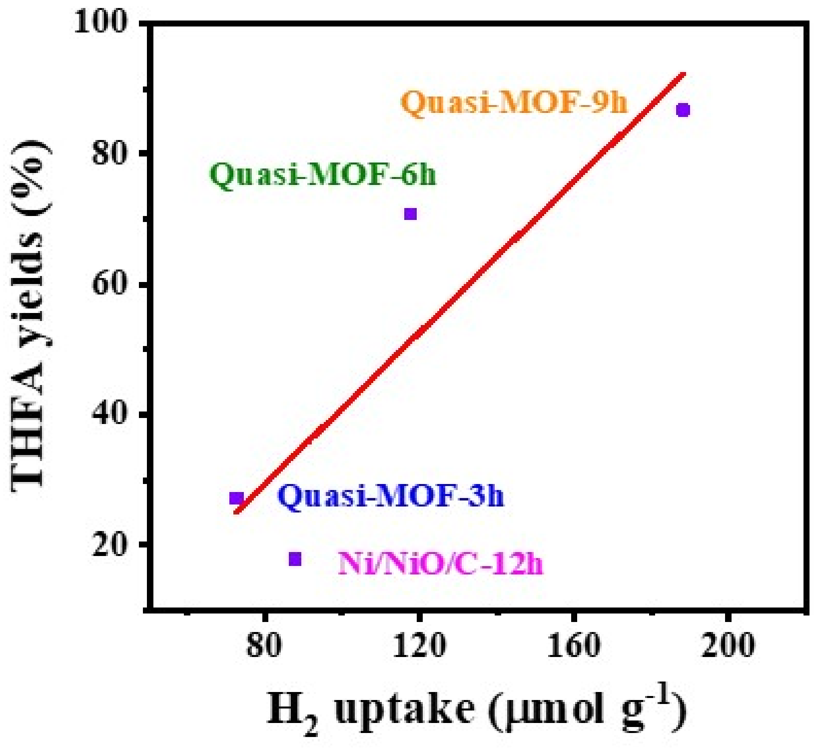

Fig. S27 Correlation between H_2 uptake and THFA yields.

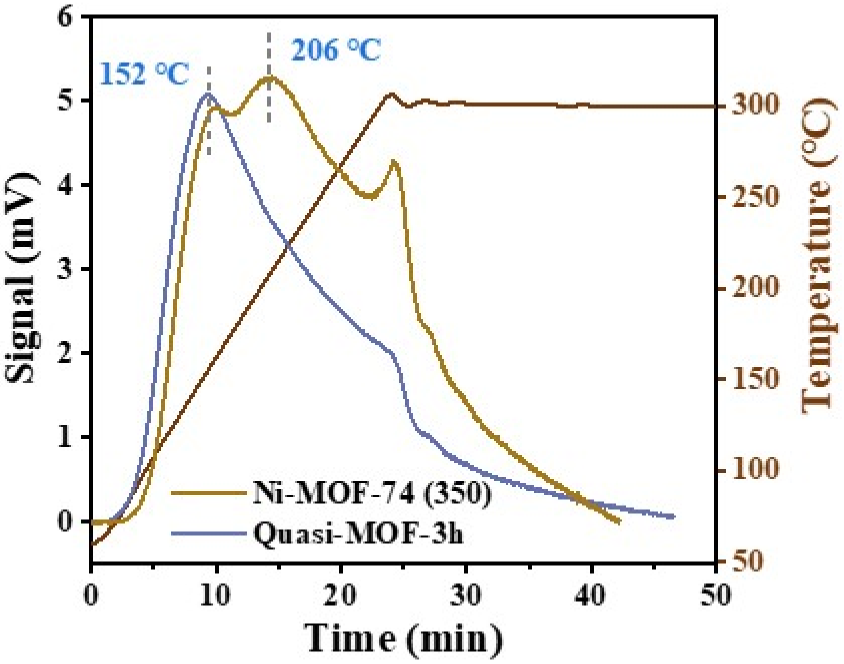

Fig. S28 H_2-TPD curves of the derivants of Quasi-MOF-3h and Ni-MOF-74(350) samples.

Table S1. Textural properties of Ni-MOF-74 and Ni-MOF-74 (T) samples

Samples	BET surface area ($m^2 \cdot g^{-1}$)	S_{micro} ($m^2 \cdot g^{-1}$)	V_{total} ($cm^3 \cdot g^{-1}$)
Ni-MOF-74	1255	1237	0.7
Ni-MOF-74 (250)	1238	1103	0.56
Ni-MOF-74 (300)	823	720	0.78
Ni-MOF-74 (350)	197	19	0.85

Table S2. Textural properties of Ni-MOF-74 derivants treated at 300 °C

Samples	BET surface area ($m^2 \cdot g^{-1}$)	S_{micro} ($m^2 \cdot g^{-1}$)	V_{total} ($cm^3 \cdot g^{-1}$)	H_2-uptake[a] ($\mu mol \cdot g^{-1}$)
Quasi-MOF-3h	823	720	0.78	87.7
Quasi-MOF-6h	563	385	0.91	117.7
Quasi-MOF-9h	261	85	1.02	188.1
Ni/NiO/C-12h	146	0	0.54	72.5

[a] calculated by H_2-TPD

Table S3. Elements analysis of the as-prepared samples (XPS results)

Samples	Element atomic (%)		
	C 1s	O 1s	Ni 2p
Quasi-MOF-3h	54.82	28.16	17.01
Quasi-MOF-6h	55.58	25.72	18.69
Quasi-MOF-9h	50.05	29.12	20.83
Ni/NiO/C-12h	42.98	31.16	25.86

Table S4. Ratio of integral areas of the Ni 2p XPS high-resolution spectrum

Ni $2p_{3/2}$ spectrum	Ni^{2+}/% (MOF)	Ni^{2+}/% (NiO)	$Ni^{2+, surf}$/%	Ni^0/%
Quasi-MOF-3h	58.85	3.74	7.50	29.90
Quasi-MOF-6h	40.38	8.26	14.03	37.33
Quasi-MOF-9h	30.93	13.40	23.92	31.74
Ni/NiO/C-12h	6.41	37.07	47.73	8.78

Table S5. Elements analysis of the as-prepared samples (ICP-OES results)

Samples	Ni contents (wt%)
Quasi-MOF-3h	36.5
Quasi-MOF-6h	50.8
Quasi-MOF-9h	55.6
Ni/NiO/C-12h	58.3

Table S6. Catalytic performance of heterogeneous catalysts for the conversion of FFR to THFA

Entry	Catalyst	FFR/Cat. (w/w)	T (°C)	P (MPa)	t (h)	Conv. (%)	Sele. (%)	Ref.
1	3% Pd/MFI[a]	11.6	220	3.4	5	100	95	1
2	Ru-MoOx[b]	2.4	100	2	1	92.1	99	2
3	Ni/C-500[a]	1	120	1	2	100	100	3
4	Cu-Ni/CNTs[c]	5.8	130	4	10	100	90.3	4
5	$Cu_1Ni_3/MgAlO$[c]	9.6	150	4	3	>99	93	5
6	Ni-LN650[b]	3.2	120	1	5	98.8	87.2	6
7	Ni-Co/SBA-15[c]	7.3	90	5	2	100	92.1	7
8	Ni@NCNTs-600-800[b]	3.2	100	4	7	100	99.5	8
9	$Ni/MMO-CO_3$[a]	5.8	110	3	3	100	99	9
10	NiCo[a]	6.7	200	8	8	100	93	10
11	$PdCo_3O_4$@NC[a]	1.4	150	2	6	100	95	11
12	NiCu[b]	2.5	140	4	4	100	95	12
13	$NiCu_{0.33}/C$[c]	67	150	3	18	100	94.6	13
14	PdNiCo/N-CNTs[c]	8	120	3	3	100	97.1	14
15	Ni(40)/MgO(30)-M[c]	2.5	140	4	4	100	100	15
16	Ni/C-400[c]	6	80	3	4	99	96.1	16
17	Ni/C-400[c]	6	80	1	4	100	98.5	17
18	Ni/TiO_2-300-450R[a]	1.9	180	2	4	100	25	18

19	Pd/LaQS[a]	1.9	120	2	0.5	100	99	[19]
20	$CuNiO_x$(1/1)-150[a]	4.8	120	3	6	100	97	[20]
21	Pd/KCC 0.3[a]	3	50	2	6	100	85	[21]
22	Quasi-MOF-9h[c]	6	70	3	4	100	98	This work

[a]2-isopropyl alcohol, [b]water, [c]ethanol

Reference:

1 N. S. Biradar, A. M. Hengne, S. N. Birajdar, P. S. Niphadkar, P. N. Joshi and C. V. Rode, *ACS Sustain. Chem. Eng.*, 2013, **2**, 272-281.

2 Y. Cao, H. Zhang, K. Liu, Q. Zhang and K. Chen, *ACS Sustain. Chem. Eng.*, 2019, **7**, 12858-12866.

3 Y. Su, C. Chen, X. Zhu, Y. Zhang, W. Gong, H. Zhang, H. Zhao and G. Wang, *Dalton Trans.*, 2017, **46**, 6358-6365.

4 L. Liu, H. Lou and M. Chen, *Int. J. Hydrogen Energy*, 2016, **41**, 14721-14731.

5 J. Wu, G. Gao, J. Li, P. Sun, X. Long and F. Li, *Appl. Catal. B*, 2017, **203**, 227-236.

6 C. Chen, R. Fan, W. Gong, H. Zhang, G. Wang and H. Zhao, *Dalton Trans.*, 2018, **47**, 17276-17284.

7 S. Li, Y. Wang, L. Gao, Y. Wu, X. Yang, P. Sheng and G. Xiao, *Microporous Mesoporous Mater.*, 2018, **262**, 154-165.

8 Wanbing Gong, Chun Chen, Haimin Zhang, G. Wang and H. Zhao, *Catal. Sci. Technol.*, 2018, **8**, 5506-5514.

9 X. Meng, Y. Yang, L. Chen, M. Xu, X. Zhang and M. Wei, *ACS Catal.*, 2019, **9**, 4226-4235.

10 J. Parikh, S. Srivastava and G. C. Jadeja, *Ind. Eng. Chem. Res.*, 2019, **58**, 16138-16152.

11 S. Pendem, S. R. Bolla, D. J. Morgan, D. B. Shinde, Z. Lai, L. Nakka and J. Mondal, *Dalton Trans.*, 2019, **48**, 8791-8802.

12 V. Sánchez, P. Salagre, M. D. González, J. Llorca and Y. Cesteros, *Molecular Catalysis*, 2020, **490**, 110956.

13 F. Tang, L. Wang, M. Dessie Walle, A. Mustapha and Y. Liu, *J. Catal.*, 2020, **383**, 172-180.

14 L. Ruan, A. Pei, J. Liao, L. Zeng, G. Guo, K. Yang, Q. Zhou, N. Zhao, L. Zhu and B. H. Chen, *Fuel*, 2021, **284**, 119015.

15 C. Sunyol, R. English Owen, M. D. González, P. Salagre and Y. Cesteros, *APPL CATAL A-GEN*, 2021, **611**, 117903.

16 D. Liu, Q. Fu, C. Feng, T. Xiang, H. Ye, Y. Shi, L. Li, P. Dai, X. Gu and X. Zhao,

Nanomaterials, 2023, **13**, 285.

17 Q. Fu, L. Yan, D. Liu, S. Zhang, H. Jiang, W. Xie, L. Yang, Y. Wang, H. Wang and X. Zhao, *Appl. Catal. B*, 2024, 343, 123501.

18 J. Zhang, D. Mao, H. Zhang and D. Wu, *APPL CATAL A-GEN*, 2023, **660**, 119206.

19 X. Zhao, Y. Wang, Z. Zhai, C. Zhuang, D. Tian, H. Guo, X. Zou and T. X. Liu, *ACS Applied Nano Materials*, 2023, **6**, 8315-8324.

20 W. Fang, S. Liu, A. K. Steffensen, L. Schill, G. Kastlunger and A. Riisager, *ACS Catal.*, 2023, **13**, 8437-8444.

21 Y. E. Kim, K.-Y. Lee and M. S. Lee, *Catal. Today*, 2024, **426**, 114392.